



# Epitope mapping of Ebola virus dominant and subdominant glycoprotein epitopes facilitates construction of an epitope-based DNA vaccine able to focus the antibody response in mice

Daniel A. J. Mitchell, Lesley C. Dupuy, Mariano Sanchez-Lockhart, Gustavo Palacios, Jaap W. Back, Katya Shimanovskaya, Sidhartha Chaudhury, Daniel R. Ripoll, Anders Wallqvist & Connie S. Schmaljohn

To cite this article: Daniel A. J. Mitchell, Lesley C. Dupuy, Mariano Sanchez-Lockhart, Gustavo Palacios, Jaap W. Back, Katya Shimanovskaya, Sidhartha Chaudhury, Daniel R. Ripoll, Anders Wallqvist & Connie S. Schmaljohn (2017) Epitope mapping of Ebola virus dominant and subdominant glycoprotein epitopes facilitates construction of an epitope-based DNA vaccine able to focus the antibody response in mice, *Human Vaccines & Immunotherapeutics*, 13:12, 2883-2893, DOI: [10.1080/21645515.2017.1347740](https://doi.org/10.1080/21645515.2017.1347740)

To link to this article: <https://doi.org/10.1080/21645515.2017.1347740>



This article not subject to US copyright law



View supplementary material [↗](#)



Accepted author version posted online: 12 Jul 2017.  
Published online: 12 Jul 2017.



Submit your article to this journal [↗](#)



Article views: 128



View related articles [↗](#)

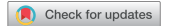


View Crossmark data [↗](#)



Citing articles: 1 View citing articles [↗](#)

RESEARCH PAPER



# Epitope mapping of Ebola virus dominant and subdominant glycoprotein epitopes facilitates construction of an epitope-based DNA vaccine able to focus the antibody response in mice

Daniel A. J. Mitchell<sup>a</sup>, Lesley C. Dupuy<sup>a</sup>, Mariano Sanchez-Lockhart<sup>a</sup>, Gustavo Palacios<sup>a</sup>, Jaap W. Back<sup>b</sup>, Katya Shimanovskaya<sup>b</sup>, Sidhartha Chaudhury<sup>c</sup>, Daniel R. Ripoll<sup>c</sup>, Anders Wallqvist<sup>c</sup>, and Connie S. Schmaljohn<sup>a</sup>

<sup>a</sup>United States Army Medical Research Institute of Infectious Diseases (USAMRIID), Fort Detrick, MD, USA; <sup>b</sup>Pepsan Presto BV, Lelystad, the Netherlands; <sup>c</sup>Biotechnology HPC Software Applications Institute, Telemedicine and Advanced Technology Research Center, US Army Medical Research and Materiel Command, Fort Detrick, MD, USA

## ABSTRACT

We performed epitope mapping studies on the major surface glycoprotein (GP) of Ebola virus (EBOV) using Chemically Linked Peptides on Scaffolds (CLIPS), which form linear and potential conformational epitopes. This method identified monoclonal antibody epitopes and predicted additional epitopes recognized by antibodies in polyclonal sera from animals experimentally vaccinated against or infected with EBOV. Using the information obtained along with structural modeling to predict epitope accessibility, we then constructed 2 DNA vaccines encoding immunodominant and subdominant epitopes predicted to be accessible on EBOV GP. Although a construct designed to produce a membrane-bound oligopeptide was poorly immunogenic, a construct generating a secreted oligopeptide elicited strong antibody responses in mice. When this construct was administered as a boost to a DNA vaccine expressing the complete EBOV GP gene, the resultant antibody response was focused largely toward the less immunodominant epitopes in the oligopeptide. Taken together, the results of this work suggest a utility for this method for immune focusing of antibody responses elicited by vaccination.

## ARTICLE HISTORY

Received 2 March 2017  
Revised 2 June 2017  
Accepted 23 June 2017

## KEYWORDS

Ebola virus; filovirus; DNA vaccine; epitope mapping; antibody; focusing; mice

## Introduction

Ebola virus (EBOV) causes severe hemorrhagic fever with a mortality rate as high as 90%. The recent epidemic in West Africa resulted in renewed efforts to develop efficacious recombinant DNA-based vaccines, most of which are based on eliciting immune responses to the major surface glycoprotein (GP) of EBOV. We previously reported the development and animal testing of filovirus DNA vaccines expressing full-length GP genes.<sup>1–3</sup> Similar to protein and whole-virus vaccination, the expression products of the DNA vaccines present a multitude of epitopes to the host immune system, many of which do not confer protective immunity. Since immunodominant epitopes are those that offer the most favorable accessibility and binding kinetics to antibodies, the immune response is skewed toward them. This phenomenon has been observed for other pathogens, with the best example being influenza virus. In this case, the influenza virus hemagglutinin 1 (HA1) globule undergoes rapid evolution under immune pressure generating poorly cross-protective immunodominant epitopes that can serve as immunological decoys.<sup>4</sup>

Here, we sought to determine if it is possible to overcome immunodominance using a defined multi-epitope DNA vaccine construct expressing both immunodominant and

subdominant gene regions. Toward this goal, we conducted a 3-part study to select and test the immunogenicity of DNA vaccine constructs encoding both immunodominant and subdominant epitopes. First, we performed epitope mapping studies using Chemically Linked Peptides on Scaffolds (CLIPS), which are able to form both linear and conformational epitopes.<sup>5</sup> We screened EBOV GP-specific monoclonal antibodies (mAbs), which recognize immunodominant epitopes. We next screened polyclonal sera from mice, guinea pigs and nonhuman primates (NHP) experimentally vaccinated against or infected with EBOV in an attempt to identify less immunodominant epitopes. Finally, we selected a subset of these epitopes to design 2 minimal epitope-based DNA vaccines. We show here that not only can such a construct focus a humoral immune response, but immunodominance can be overcome due to epitope availability within the construct.

## Results

### CLIPS libraries

A general description of CLIPS technology and types of scaffolds used in screenings has been described previously.<sup>5</sup> A total

**CONTACT** Connie S. Schmaljohn  [connie.s.schmaljohn.civ@mail.mil](mailto:connie.s.schmaljohn.civ@mail.mil)  U.S. Army Medical Research Institute of Infectious Diseases, 1425 Porter Street, Frederick, MD 21769, USA.

 Supplemental data for this article can be accessed on the [publisher's website](#).

This article not subject to US copyright law

This is an Open Access article distributed under the terms of the Creative Commons Attribution-NonCommercial-NoDerivatives License (<http://creativecommons.org/licenses/by-nc-nd/4.0/>), which permits non-commercial re-use, distribution, and reproduction in any medium, provided the original work is properly cited, and is not altered, transformed, or built upon in any way.

of 7,286 different CLIPS peptides derived from the EBOV GP-1 and GP-2 amino sequences were synthesized on scaffolds and placed into 14 different groups for screening. Group 1 included overlapping looped 15-mers, and Group 2 comprised overlapping linear 15-mers. The remaining groups consisted of 21-mer or 32-mer peptides constructed from 9-mers separated by 2 cysteine residues and additional terminal cysteine residues to allow disulfide bond formation. Each 9-mer in the sequence was paired with sequential 9-mers across the GP amino acid sequence resulting in a peptide library that was intended to simulate both linear and conformational epitopes.<sup>5</sup> For fine mapping of specific antigenic regions of EBOV GP, a series of 6,518 additional CLIPS peptides were generated based on the initially retrieved leads. These fine mapping variants include all proteogenic amino acid substitutions at each amino acid position within putative epitopes to allow assessment of the individual residue contributions to the epitopes.

### Epitope mapping with murine antibodies

The CLIPS libraries were probed with murine mAbs 13F6, 13C6, 6D8 and 6E3<sup>6</sup>. As described previously, all 4 of these mAbs were found to provide partial protection against EBOV challenge when passively transferred to BALB/c mice. mAbs 13F6 and 6E3 are in the same competitive binding group (Group 1), but have different isotypes (IgG1 or IgG2a, respectively). Neither of these mAbs neutralized EBOV in cell culture

assays.<sup>6</sup> mAbs 6D8 and 13C6 are in different competitive binding groups (2 and 4, respectively) and both were shown to neutralize EBOV in cell culture assays in the presence of complement.<sup>6</sup> Polyclonal sera tested included archived samples from previous studies.

Initial screening showed that mAb 13F6 binds to peptides in groups 1, 2, 7, and 13 (Figure S1). Fine mapping by full substitution mutagenesis revealed clear binding to the amino acid region  $_{391}\text{TPVYKLDISEATQVEQHRRRTDNDNS}_{415}$  with  $_{406}\text{QHRRRTD}_{412}$  as core of the epitope and the motif  $_{406}\text{QXXRXT}_{411}$  being most essential (Fig. 1A). Similarly, mAb 6E3, which was previously found to be in the same competition group as mAb 13F6<sup>6</sup>, bound to this same region, and full substitution mutagenesis revealed that the core of the epitope was  $_{406}\text{QHRRRTD}_{412}$  with  $_{406}\text{QXHRR}_{410}$  as the most important residues (Fig. 1B). The mAb 6D8 also bound to CLIPS peptides having the amino acid sequence  $_{391}\text{TPVYKLDISEATQVEQHRRRTDNDNS}_{415}$ , and full substitution mutagenesis showed that  $_{394}\text{YKLDI}_{398}$ , was the core of the epitope with  $_{395}\text{KLD}_{397}$  as the most essential amino acids (Fig. 1C).

Negative control sera from naïve mice or mice vaccinated with an empty vector DNA vaccine showed no binding in the CLIPS screening (data not shown). Positive control sera included pooled sera from mice that had been vaccinated with either a wild-type EBOV GP DNA vaccine (initial screening) or a codon-optimized GP DNA vaccine (fine mapping). Both of these GP DNA vaccine constructs were

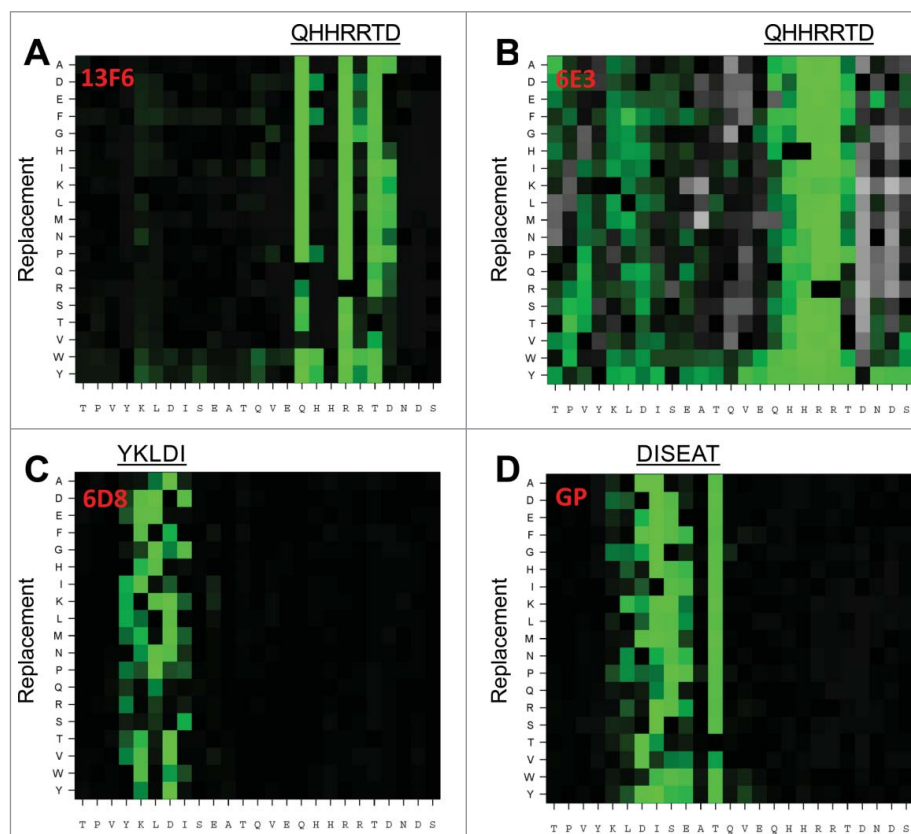


**Figure 1.** Antibody binding after full substitution mutagenesis of  $_{391}\text{TPVYKLDISEATQVEQHRRRTDNDNS}_{415}$ . Substituted amino acids are shown on the right side of each heat map. Green indicates significantly reduced binding. (A) The core of the mAb 13F6 epitope was determined to be  $_{406}\text{QHRRRTD}_{412}$ , with  $_{406}\text{QXXRXT}_{411}$  being most essential for binding. (B) The core of mAb 6E3 was also  $_{406}\text{QHRRRTD}_{412}$ , with  $_{406}\text{QXHRR}_{410}$  most essential to binding. (C) The core of the epitope for mAb 6D8 was determined to be  $_{394}\text{YKLDI}_{398}$ , with  $_{395}\text{KLD}_{397}$  as the most essential amino acids. (D) Polyclonal sera from mice vaccinated with WT GP of EBOV showed strongest binding to  $_{397}\text{DISEAT}_{402}$ , with  $_{398}\text{ISXXT}_{402}$  as the most crucial amino acids.

previously found to protect mice from challenge with EBOV, but the optimized construct displayed improved expression in cell culture.<sup>2</sup> In the initial CLIPS screening, we found that the positive control sera bound to peptides in groups 1, 2, 3, and 13 (Figure S2). Positional scanning showed <sub>397</sub>DISEAT<sub>402</sub> to be the core of the epitope recognized, with <sub>398</sub>ISXXT<sub>402</sub> as the most crucial amino acids (Fig. 1D). In addition to this region, we also observed lesser binding by the polyclonal WT GP DNA-vaccinated mice to <sub>41</sub>STLQVSDVDKLVCRDKLLSSTNMLRS<sub>65</sub> and <sub>197</sub>HPLREPVNATED<sub>206</sub> (data not shown).

We also screened the CLIPS libraries with a serum sample from mice that were vaccinated with the Venezuelan equine encephalitis virus replicon particle (VRP)-based EBOV GP vaccine that was originally used to generate the mouse mAbs in this study and that survived challenge with EBOV.<sup>6</sup> As with sera from mice vaccinated with the GP DNA vaccines (but not challenged), sera from the VRP-vaccinated and EBOV challenged survivor showed strong binding to <sub>391</sub>TPVYKLDISEATQVEQHRRRTDNDNS<sub>415</sub> and positional scanning of the VRP survivor showed <sub>395</sub>KLDI<sub>398</sub> as the core of the epitope (data not shown) similar to what was observed for mAb 6D8. In total, our CLIPS screening data with murine antibodies indicated that this region of the mucin-like domain, which includes the epitope binding regions for mAbs 13F6, 6E3, and 6D8, is highly immunodominant in mice.

The results obtained with mAbs 13F6, 6E3 and 6D8, were consistent with earlier studies; however, our results using mAb 13C6 were not. Our initial screening with mAb 13C6 showed

binding to CLIPS peptides in Groups 1, 2, 7, 12, and 13 (Figure S3). The mAb 13C6 epitope is conformational and binds to both GP1 and sGP.<sup>6</sup> The epitope for this mAb has been reported to reside in the glycan cap region of GP1, a region containing 6 N-linked glycosylation sites, which is believed to shield the receptor binding domain.<sup>7-9</sup> Our CLIPS binding results differ from this finding, and instead show binding to a region near epitopes for mAbs 12B5<sup>6</sup> and 14G7<sup>6</sup>. We repeated the experiment using a different aliquot of mAb 13C6, which was derived from a separate hybridoma subclone, with the same results. We also compared the productive IGH rearranged nucleotide sequences from the 2 clonal derivatives (13C6 1.1 and 13C61.1.1) and found them to be identical to one another and to the original reported nucleotide sequences for 13C6 (data not shown). To further investigate our findings with mAb 13C6, we generated phage libraries displaying WT EBOV GP peptides as described previously.<sup>10</sup> This library was constructed to display 50-mer long peptides from EBOV GP at the end of the T7 capsid, with a sliding window of 10 amino acids from the previous peptide. Panning with mAb 13C6 enriched phages displaying <sub>461</sub>NNNTHHQDTGEESASSGKLG<sub>500</sub>GLITNTIAGVAGLITGRRRTR peptide, which includes the same region (underlined) identified with CLIPS. This region also includes the epitope for mouse mAbs 12B5 and 14G7.<sup>6,11</sup>

To explore the residues that contribute most to the mAb 13C6 binding, we performed positional scanning with mAb 13C6 in comparison to mAb 6D8. As expected, mAb 6D8 bound to <sub>391</sub>TPVYKLDISEATQVEQHRRRTDNDNS<sub>415</sub>, and substitutions for residues <sub>394</sub>YKLDI<sub>398</sub> negatively impacted

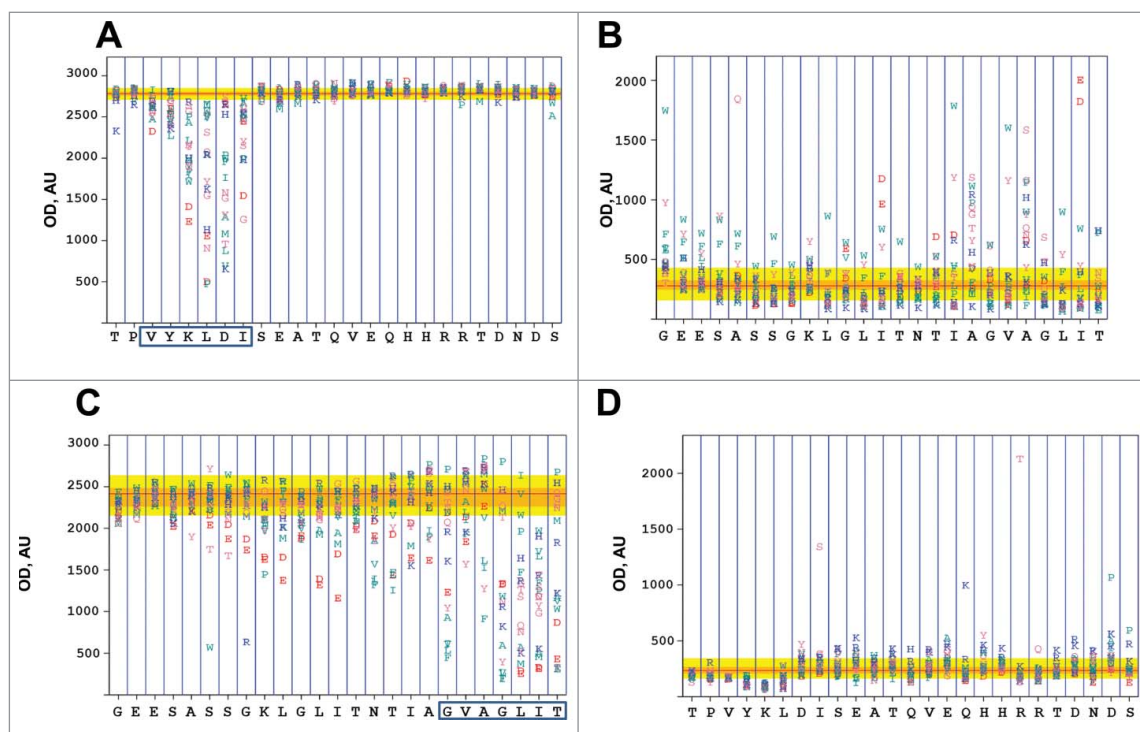


**Figure 2.** Full substitution mutagenesis of mAbs 13C6 and 6D8. The letter plots depict pepscan results for each peptide on the X axis with recorded intensities (optical density, OD) expressed in arbitrary units (AU) plotted on the Y axis. (A) Binding of mAb 6D8 to a full series of substitutions of <sub>391</sub>TPVYKLDISEATQVEQHRRRTDNDNS<sub>415</sub> indicates decreased binding upon mutations to <sub>393</sub>VYKLD<sub>397</sub> (boxed), which is thought to be the epitope core. (B) Binding of mAb 6D8 to a full substitution series of <sub>470</sub>GEESASSGKLG LITNTIAGVAGLIT<sub>494</sub> indicates no binding to this stretch of amino acids. (C) Binding of mAb 13C6 to a full substitution series of <sub>470</sub>GEESASSGKLG LITNTIAGVAGLIT<sub>494</sub> indicates decreased binding upon mutations to <sub>487</sub>GVAGLIT<sub>493</sub> (boxed) and appears to be generally sensitive to introduction of negative charges into the peptides. (D) Binding of mAb 13C6 to a full substitution series of <sub>391</sub>TPVYKLDISEATQVEQHRRRTDNDNS<sub>415</sub> indicates no binding to this stretch of amino acids.

binding (Fig. 2A). Also as expected, mAb 6D8 did not bind to the <sub>470</sub>GEESASSGKLGITNTIAGVAGLIT<sub>494</sub> region identified for mAb 13C6 binding (Fig. 2B). Conversely, mAb 13C6 bound poorly to the mAb 6D8 epitope <sub>391</sub>TPVYKLDISEATQVEQHRRRTDND<sub>415</sub> (Fig. 2C), but bound strongly to <sub>470</sub>GEESASSGKLGITNTIAGVAGLIT<sub>494</sub> (Fig. 2D). The residues that contribute most to mAb 13C6 binding in this assay are those comprising the motif on the end of this peptide: <sub>487</sub>GxAGLIT<sub>494</sub>. Of note, introduction of a negatively charged residue (D or E) at any point disturbed binding (Fig. 2D).

### Comparison of epitopes bound by a variety of experimentally vaccinated or infected mice, guinea pigs or NHP

To attempt to identify additional EBOV epitopes for inclusion in the multi-epitope constructs, we performed CLIPS screenings using sera from mice and guinea pigs experimentally vaccinated against EBOV but not challenged and from rhesus macaques that were not vaccinated, but had been treated with antiviral drugs and survived EBOV infection.<sup>12,13</sup> These studies were intended to ascertain if varying the antigenic presentation of GP with different types of vaccines, or by infection with EBOV without prior vaccination, resulted in antibody responses to unique epitopes. Sera tested included pooled sera from mice vaccinated with a WT EBOV GP DNA vaccine, negative control samples from mice vaccinated with the empty vector DNA vaccine, and sera from mice vaccinated with DNA constructs in which one or the other of the 2 GP2 N-linked glycosylation sites were mutated as described previously.<sup>14</sup> In our earlier studies, we found that mutating <sub>563</sub>NET<sub>565</sub> to <sub>563</sub>AET<sub>565</sub> (MUTC, Fig. 3) resulted in GP2 that did not co-precipitate with GP1 and that had reduced immunogenicity and protective efficacy in

mice. In contrast, mutating <sub>618</sub>NIT<sub>620</sub> to <sub>618</sub>AIT<sub>620</sub> (MUTD, Fig. 3) resulted in GP2 that still co-precipitated with GP1 and minimally impacted elicitation of protective immunity.<sup>14</sup> Consequently, we reasoned that these sera might recognize different GP epitopes than sera from mice vaccinated with WT EBOV GP DNA vaccines. The 2 pooled guinea pig serum samples were from earlier EBOV DNA vaccine studies (unpublished), both of which were collected 21 d after the final vaccination, but before challenge with EBOV. Sample 107 (Fig. 3) came from guinea pigs vaccinated by gene gun with an EBOV DNA vaccine expressing both the GP and NP genes of EBOV<sup>15</sup> and boosted with recombinant baculovirus generated GP.<sup>3</sup> Sample 130 (Fig. 3) came from guinea pigs vaccinated with the EBOV GP DNA vaccine and boosted with a recombinant vaccinia virus expressing EBOV GP (unpublished).

Like samples from mice vaccinated with the WT EBOV GP DNA vaccine (Fig. 1 and S3), CLIPS screening of pooled sera from mice that had been vaccinated with MUTD DNA showed strong binding to CLIPS peptides containing <sub>391</sub>TPVYKLDLIS<sub>399</sub>, whereas samples from MUTC vaccinated mice did not (Fig. 3 and S5). One of the guinea pig samples (130, Fig. 3) and one of the rhesus macaque samples (C250B, Fig. 3) also showed strong binding to this region of GP. Sera from mice vaccinated with MUTC and MUTD, but not with WT GP DNA vaccines, bound strongly to <sub>43</sub>LQVSDVDKLVCRDKL<sub>57</sub> (Fig. 3), suggesting that the mutant DNA vaccines were eliciting different antibody responses. This same region was also recognized by one of the guinea pig samples (130, Fig. 3). The 2 guinea pig samples also recognized several epitopes that were not strongly bound by antibodies in the polyclonal mouse sera, but were bound by rhesus macaque sera (Fig. 3). Only 2 of the rhesus macaque sera (R1510 and

	Amino Acid #	Amino Acid Sequence	Mouse				Guinea Pig		Rhesus Macaque							
			WT GP	MUTC	MUTD	Vector	107	130	H117X	AXXX	L2012	R1510	C573	C250B	Vector	
GP1 core 1-190	43-57	LQVSDVDKLVCRDKL														
	84-99	KRWGFRSGVPPKVVNY														
	111-120	YNLEIKKPDGSE														
	192-210	DFSSHPLREPVNATEDPS														
Glycan cap 227-313	249-274	TIYTSGRSNTTGKLI														
	283-297	TTIGEWAFWETKKNL														
	311-323	VSNAGKNISGGSP														
	332-350	TNITTEDHKIMASESSAM														
	352-365	QVHSQGREAAVSHL														
	368-388	LATISTSPQSLTTKPGPDNST														
	391-399	TPVYKLDIS														
	397-405	DISEATQVE														
Mucin-like 313-464	405-414	EQHRRRTDND														
	412-421	DNDSTADTP														
	429-443	PPKAENTNTSKSTDF														
	439-448	KSTDFLDPAT														
	448-462	TTTSPQNHSETAGNN														
	463-477	NTHHQDTGEESASSG														
	475-486	SSGKLGITNTI														
Furin cleavage 497-501	480-494	GLITNTIAGVAGLIT														
	492-501	LITGRRRTRR														
	561-576	LANETQALQ LFLRAT														
	572-583	FLRATTELRTFS														
GP2 502-676	582-594	FSILNRKAIDFLI														
	632-640	DKTLPDQGD														
	634-647	TLPDQGDNDNWWTG														

Figure 3. Relative binding of serum samples from mice, guinea pigs and rhesus macaques to amino acids in CLIPS. Blue indicates strong binding and tan indicates weaker binding. No color indicates no measurable binding with that particular sample.

C250B, Fig. 3) bound strongly to epitopes in GP2, although weaker binding was also noted for mouse and guinea pig samples (Fig. 3).

### Construction of epitope-based DNA vaccines

Using the CLIPS data and structural modeling based on the initial X-ray crystal structure of EBOV GP,<sup>16</sup> we sought to determine if it is possible to present the immune system with both immunodominant and subdominant epitopes and generate immune responses to all of them. As representative immunodominant epitopes, we included gene regions encoding the epitopes for mouse mAb 6D8 (<sub>392</sub>PVYKLDISEA<sub>401</sub>), and mAbs 13F6 and 6E3 (<sub>406</sub>QHHRRT<sub>411</sub>). We also included the gene region encoding <sub>477</sub>GKLGLITN<sub>484</sub>, because in CLIPS screening this epitope was recognized strongly by sera from guinea pigs and rhesus macaques (Fig. 3). Also, this region encodes the amino acids in the 2 overlapping peptides that were originally shown to be recognized by mouse mAbs 12B5 and 14G7 (<sub>477</sub>GKLGLITNTIAGVAGLI<sub>493</sub>)<sup>6,11</sup> (mAb 12B5 (partial), Table 1), as well as in our CLIPS and phage display screenings with mAb 13C6 (Fig. 2 and S4). Multi-epitope construct 1 (Mep1) was designed to also include 2 subdominant epitopes that were predicted to be accessible on the surface of EBOV GP (M1 & M2, Fig. 4), one of which (<sub>88</sub>FRSGVPPK<sub>95</sub>) was weakly recognized in CLIPS screenings using guinea pig and rhesus macaque sera and the other of which (<sub>111</sub>LEIKKPDG<sub>118</sub>) was not recognized by any of the immune sera (Fig. 3). There was no linker between the signal peptide and the M1 epitope in Mep1, but all of the other epitopes were separated by flexible linkers consisting of 4 glycine residues (Table 1). This construct also included the N-terminal EBOV signal peptide (33 amino acids) preceding the epitopes to facilitate intracellular trafficking. The EBOV transmembrane domain was included to anchor the construct to the cell surface (Table 1).

Like Mep1, Mep2 contained the EBOV signal peptide, but differed from Mep1 in that it also encoded the first 7 amino acids of the N-terminus of GP1 (Table 1). These 7 amino acids were included to potentially enhance signal peptide removal before a glycine linker, which was inserted before each epitope.

Mep2 was intended to generate a secretion product as it did not have a transmembrane domain. The same 3 immunodominant epitopes as in Mep1 were included in Mep2, which were followed by 2 linear epitopes that were predicted to be surface accessible on EBOV virions (M3 & M4, Fig. 4), but did not appear to be immunodominant in mice vaccinated with the WT EBOV GP DNA vaccine. One of these (M3) is the epitope that was bound by antibodies in sera from mice vaccinated with the 2 glycosylation mutants and one of the guinea pig pools (<sub>45</sub>VSDVDKLVCRDKL<sub>57</sub>), but not by sera from mice vaccinated with the WT EBOV GP DNA vaccine (Table 1 and Fig. 3). The other (M4, Fig. 4) is an epitope recognized by both guinea pig sera and one of the rhesus macaque sera in the CLIPS screen (<sub>195</sub>SSHPLREPV<sub>203</sub>), but was not strongly bound by any of the mouse samples (Fig. 3). Mep2 also included 2 putative conformational epitopes which were the strongest binders identified by CLIPS screening with the pooled sera from mice vaccinated with the WT GP DNA vaccine (Figure S2, Group-13). These CLIPs both consisted of simple double-loop structures with the linear, protective, neutralizing epitope of mAb 6D8 followed by 2 C residues to allow disulfide bonding and one of 2 overlapping regions from the mucin-like domain (<sub>433</sub>ENTNTSKG<sub>441</sub> or <sub>427</sub>AGPPKAENT<sub>435</sub>).

Both Mep constructs produced polypeptides recognized by mAb 6D8 when assayed by immunofluorescent antibody staining of transfected cells (Fig. 5A). As expected, ELISA of cell culture supernatants from transfected cells demonstrated that Mep2, but not Mep1 produced a secreted expression product (Fig. 5B). Western blots of a Mep1 cell lysate with mAb 6E3 or Mep2 cell supernatant with mAb 6D8 showed expression products of the expected sizes (data not shown).

### Mouse immunogenicity and immune focusing

To evaluate the immunogenicity of the epitope constructs, we vaccinated groups of 10 mice with the Mep1 or Mep2 DNA vaccines 3 times at 3-week intervals using intramuscular electroporation. Blood samples collected at day 0 and 3 weeks after each vaccination were analyzed by ELISA using whole EBOV antigen. Mep1 elicited no detectable antibody response after 2

**Table 1.** Predicted features and amino acid compositions of expression products encoded by the Mep1 and Mep2 DNA vaccines.

<b>Mep1</b>				
Epitope	Predicted Features	Predicted Amino Acid Sequence	Linker	Amino Acids
SP	Signal peptide	MGVTGILQLPRDRFKRTSFFLWVILFQRTFSI	none	1–33
M1	Linear- Accessible	FRSGVPPK	GGGG	88–95
M2	Linear- Accessible	LEIKKPDG	GGGG	111–118
MAb6D8	Linear- mucin	PVYKLDISEA	GGGG	392–401
MAb13F6	Linear- mucin	QHHRRT	GGGG	406–411
MAb12B5 (partial)	Linear- mucin	GKLGLITN	GGGG	477–484
TM	transmembrane domain	WIPAGIGVTGVIIAIVIALFCICKFVF	none	651–676
<b>Mep2</b>				
Epitope	Predicted Features	Predicted amino acid sequence	linker	Amino Acids
SP-GP1	Signal peptide	MGVTGILQLPRDRFKRTSFFLWVILFQRTFSI -PLGVIHN	GGGG	1–40
MAb6D8	Linear- mucin	PVYKLDISEA	GGGG	392–401
MAb13F6	Linear- mucin	QHHRRT	GGGG	406–411
MAb12B5 (partial)	Linear- mucin	GKLGLITN	GGGG	477–484
M3	Linear	VSDVDKLVCRDKL	GGGG	45–57
M4	Linear	SSHPLREPV	GGGG	195–203
Conf-1	Conformational-mucin	CTPVYKLDISCCENTNTSKGTC	GGGG	391–399_433–441
Conf-2	Conformational-mucin	CTPVYKLDISCCAGPPKAENTC	GGGG	91–399_427–435

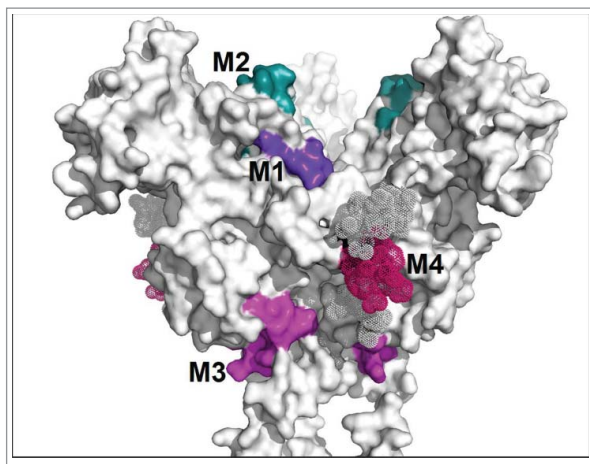


**Figure 4.** EBOV GP structural modeling. A surface model representation of the EBOV GP trimer is shown in white. The 3D representation omits the mucin-like domain in GP, which is considered unstructured. Smooth regions of the surface highlight the parts of the structure that were determined through X-ray crystallography.<sup>25</sup> Other portions of the structure that were not resolved experimentally have been modeled “de novo” and are shown as collections of dots to indicate the approximate location of the missing fragments. Epitopes M1 to M4 identified in the CLIPS study and included in the multi-epitope constructs described in Table 1 are highlighted in purple, blue, magenta and red, respectively.

vaccinations and only a low response after 3 vaccinations (Fig. 5C). Mep2 elicited a detectable response after 2 vaccinations with a rise in ELISA antibody titer after 3 vaccinations (Fig. 5C). Consequently, to determine if the multi-epitope constructs could influence immunodominance, we used Mep2 to

vaccinate mice either alone or as a boost to WT GP. We assessed antibody responses by ELISA using peptides that contained the epitopes of interest (Table S1).

Sera from mice vaccinated once with the WT GP DNA vaccine had low antibody responses to peptides corresponding to epitope M4 as well as those recognized by mAbs 6D8 and 13F6 (Fig. 6A). After 3 vaccinations with WT GP, additional responses to the other peptides excluding those representing epitope M3 were also detected, with antibodies raised to WT GP showing the strongest responses to peptides 65, which includes the <sup>394</sup>YKLDI<sub>398</sub> epitope identified by positional scanning with mAb 6D8, and peptide 67, which includes the <sup>406</sup>QHRRRTC<sub>412</sub> epitope identified by positional scanning with mAbs 13F6 and 6E3 (Fig. 6B). In contrast, 3 vaccinations with Mep2 elicited strong responses to the subdominant epitopes M3 and M4 represented by peptides 7, 8, and 32, 33, respectively (Fig. 6C). Mep2 elicited weak to no responses to the immunodominant epitopes identified for mAbs 6D8, 6E3 and 13F6, which were represented by peptides 65, 66, 67, 68, and 69. When mice were vaccinated once with the WT GP DNA vaccine followed by 2 booster vaccinations with Mep2, strong responses to peptides representing M3 and M4 were observed, as well as a moderate response to peptides representing epitopes for mAbs 6D8, 13F6 and 12B5 (Fig. 6D). These data suggest that the Mep2 construct is able to skew the immune response of the WT GP DNA vaccine toward subdominant epitopes found in the WT GP construct.

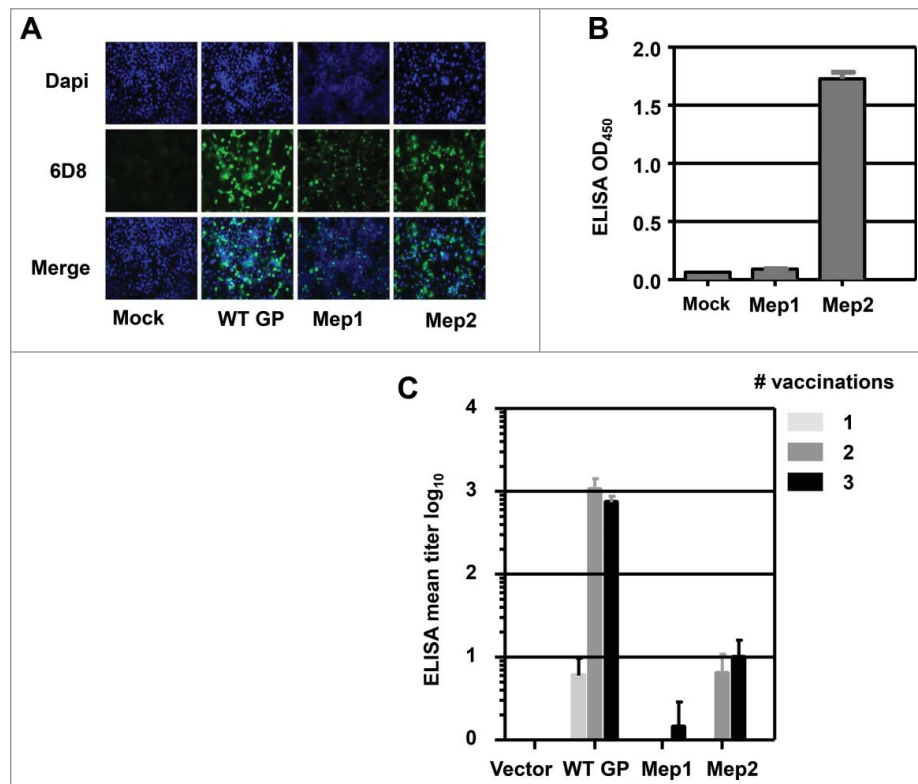


**Figure 5.** Mep 1 and Mep2 expression. (A) Cells were transfected with the Mep1 or Mep2 DNA vaccine constructs or with the WT GP DNA vaccine and stained with DAPI (top panels). Immunofluorescent antibody staining was performed with EBOV mouse mAb 6D8 (middle panels). Lower panels show a merge of the top and middle panels. (B) ELISA was performed on cell supernatants of mock-transfected cells or cells transfected with the Mep1 or Mep2 constructs. (C) Groups of mice ( $N = 10$ ) were vaccinated 3 times with empty plasmid vector, the WT GP DNA vaccine, or the Mep1 or Mep2 constructs. ELISA was performed on serum samples obtained 3 weeks after each vaccination using inactivated EBOV virions as antigen.

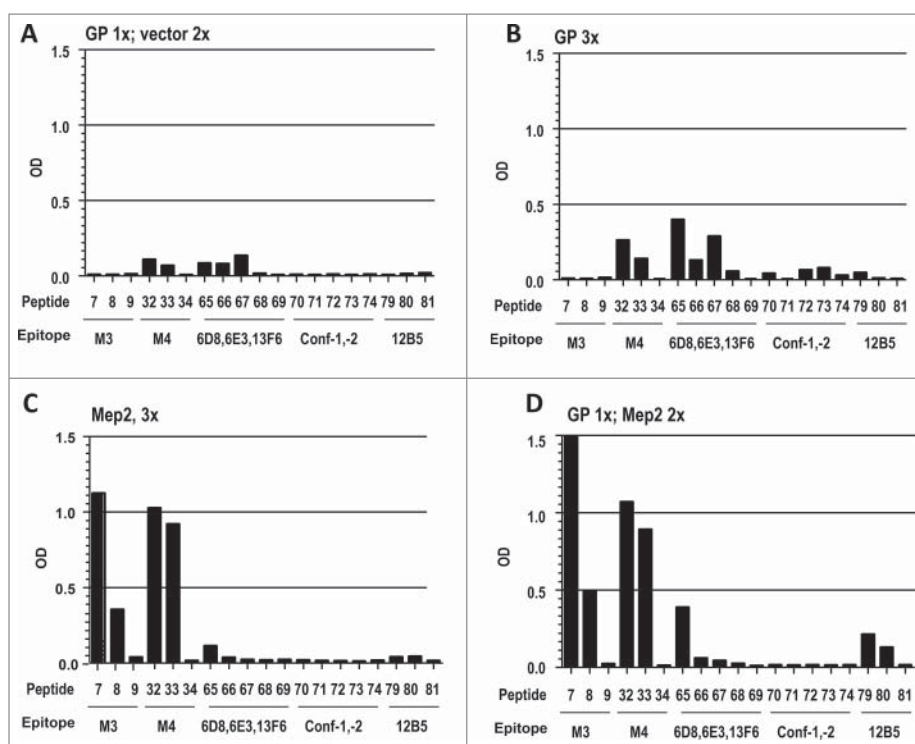


**Figure 6.** ELISA using linear peptides containing epitopes included in Mep2. Linear peptides are as defined in Table 1 and Table S1. The epitopes contained in part or in whole in each of the peptides are identified beneath the peptide numbers. (A) Samples from mice vaccinated once with the WT GP DNA vaccine followed by 2 vaccinations with an empty plasmid vector control; (B) samples from mice vaccinated 3 times with the WT GP DNA vaccine; (C) samples from mice vaccinated 3 times with the Mep2 DNA vaccine; and, (D) samples from mice vaccinated once with the WT GP DNA vaccine followed by 2 vaccinations with the Mep2 DNA vaccine.

To investigate the possibility that antibody focusing toward M3 and M4 was due to inclusion of strong T-helper epitopes in Mep2, we searched for potential T-cell epitopes using the Immune Epitope Database and Analysis Resource (<http://www.iedb.org/>). The Mep1 and Mep2 constructs both had very poor overall scores, with the best score observed for the 6D8 epitope (score  $\geq 5.54$ ). For comparison, the M3 and M4 epitopes have much poorer scores ( $>32$  and  $>42$ , respectively). Consequently, the reason for the immune focusing toward the subdominant epitopes M3 and M4 when Mep2 was used to boost GP primed mice is not likely to be due to the inclusion of strong Th epitopes in Mep2, within the predictive bounds of the capability of the epitope search programs.

## Discussion

In this study, we evaluated epitope-specific antibody responses to EBOV GP using CLIPS libraries probed with mouse mAbs, which were previously found to provide protection against EBOV challenge in mice,<sup>6</sup> and with polyclonal antibody samples from experimentally vaccinated or infected animals. The neutralizing mAbs, 13C6 and 6D8 represent different competition groups whereas the non-neutralizing mAbs 13F6 and 6E3 were in the same competition group but had different isotypes. These mAbs, therefore, allowed for the possible selection of distinct epitopes that could be involved in protection from EBOV by differing mechanisms. In a recent study of EBOV mAbs, including 13C6, cooperativity between non-neutralizing and neutralizing mAbs was observed.<sup>17</sup> For example, mAb 13C6, which neutralizes EBOV and also binds weakly to Sudan virus

(SUDV) GP, was found to show increased binding to SUDV GP in the presence of the non-neutralizing mAb FVM20.<sup>17,18</sup> In that study, it was postulated that mAb cooperativities might be related to “induced epitopes” formed or exposed by the binding of another antibody. Thus, it is possible that a construct containing both neutralizing and non-neutralizing epitopes would be superior to constructs with only neutralizing epitopes.

For the mouse mAb 13F6, the residues <sub>406</sub>QXXRXT<sub>411</sub> were found to be crucial to the core of the epitope, which is in agreement with a recent alanine scanning study that implicated Q406, R409, T411, and D412 as crucial to epitope binding.<sup>19</sup> Likewise, CLIPS screening with mAb 6E3 defined the crucial residues for binding to be <sub>406</sub>QXHRR<sub>410</sub>. This slight difference in the critical binding residues defined for mAbs 6E3 and 13F6 augment earlier findings indicating that they also differ in isotype (IgG1 vs. IgG2a, respectively) and ability to confer passive protection in mice.<sup>6</sup> CLIPS screening and positional mapping of the mAb 6D8 epitope, which identified residues <sub>395</sub>KLD<sub>397</sub> as critical for binding, agrees with other studies,<sup>6,19</sup> but further delineates this epitope. In contrast, our results with mAb 13C6 do not correlate with those from earlier structural studies, which clearly show that mAb 13C6 binds to the glycan cap region of EBOV GP.<sup>19-22</sup> In our studies, both CLIPS libraries identified a binding region for mAb 13C6 just outside the mucin-like domain and before the furin cleavage site for GP1 and GP2 and in the same region bound by mAbs 12B5 and 14G7.<sup>6</sup> Panning of a phage display library identified the same binding region as the CLIPS libraries, and full mutagenesis scanning corroborated these results and indicated that substitutions to <sub>487</sub>GxAGLIT<sub>494</sub> negatively correlate with binding.

Although we have not determined the reason for the discrepancies between our results and the structural data, of note is that our work was performed using the original mouse mAb 13C6,<sup>6</sup> whereas the structural studies used a chimeric human/mouse mAb produced in plants.<sup>22</sup> Differences in the heavy chains of mouse mAb 4G7 and the analogous chimeric mAb c4G7 were postulated to explain differences in binding observed in structural studies.<sup>22</sup> Alternatively, what we observed could be due to promiscuous binding of mAb 13C6. One possibility is that the CLIPS studies are detecting the peptide <sub>475</sub>SSGKL<sub>479</sub> rather than <sub>270</sub>TTGKL<sub>273</sub> in the glycan cap as in the electron microscopy (EM) studies.<sup>22</sup> The T residues in the epitope identified in the EM structure form a tight loop that goes deep in the antibody binding pocket of mAb 13C6. On the other hand, our positional scanning (Fig. 2) shows that T residues replacing both S residues in <sub>475</sub>SSGKL<sub>479</sub> are the most unfavorable of the amino acid changes possible. In other words, the conformation of the <sub>270</sub>TTGKL<sub>273</sub> fragment found in the GP/sGP structure is not a favorable one on the oligopeptides, and the loop in the X-ray structure is probably forced during the folding process of GP. It would be interesting to perform a structural study with mAb 13C6 and these linear epitopes, similar to the study already reported for mAb 14G7<sup>11</sup> and its linear peptide epitope, which resides in the same region of the mucin-like domain that we identified for mAb 13C6.

Other interesting, but unsurprising findings from our CLIPS screenings were the differing epitopes recognized by antibodies in polyclonal sera of vaccinated or infected mice, guinea pigs and rhesus macaques. Clearly, the small number of samples that we screened prevent generalizations about immunodominant epitope differences, but they do hint that there are both highly immunodominant epitopes on GP that are frequently recognized by all species tested as well as epitopes that might be more commonly recognized by specific species or when comparing vaccinated versus infected animal samples.

For the purposes of our work, we chose epitopes recognized by mouse mAbs 6D8, 13F6 and 12B5, but did not include that of mAb 13C6 due to the discordant mapping results, as the immunodominant portions of our constructs. We also selected 4 accessible but subdominant epitopes to combine with these to determine if the immunodominant epitopes would obstruct the generation of broad immunity. Although both the Mep1 and Mep2 constructs produced intracellular oligopeptides recognized by IFA with EBOV mAbs, the Mep2 expression appeared to be stronger. More importantly, Mep1 was poorly immunogenic in mice. We suspect the poor immunogenicity of Mep 1 was related to the transmembrane domain, which was intended to allow cell surface presentation of the epitopes. It is possible that this anchoring did not provide adequate presentation to the mouse immune system or that the oligopeptide did not assume a favorable conformational structure to elicit strong antibody responses in mice. Alternatively, cleavage of the signal peptide or intracellular trafficking might have been suboptimal due to the amino acids of the first epitope, which are different from those of authentic EBOV GP. To eliminate these potentially negative impacts on immunogenicity, we designed our second construct, Mep2, to encode the signal peptide followed by the first 7 N-terminal residues of GP1 and a 4 glycine linker before the first epitope. We also eliminated the transmembrane

coding region to promote secretion of the expression product. Mep2 was found not only to have better intracellular expression than Mep1, but also was secreted and elicited a much better antibody response than Mep1 in vaccinated mice.

When Mep-2 was used as a boost to WT GP, the responses skewed to the subdominant epitopes in Mep2. We did not detect antibody responses to 2 peptides designed as simple double-loop structures including the linear protective epitope of mAb 6D8; however, we do not know if these epitopes folded correctly or were presented effectively to elicit an antibody response. Currently, we do not have a mechanistic explanation for the immune-focusing that we observed with Mep2. One possibility would be that strong T-helper epitopes were present in the construct that were capable of promoting a robust response to these epitopes. However, this is apparently not the reason, as T-cell epitopes predicted within the sub-dominant M3 and M4 domains were very weak whereas the class II-restricted epitopes in the dominant 6D8 epitope were much stronger. Another possibility is that the prediction programs do not adequately identify all strong T-cell epitopes. Clearly, additional studies would be required to determine how Mep2 is able to refocus the antibody response toward these subdominant epitopes.

In conclusion, our data suggest that it is possible to use a multi-epitope DNA vaccine construct to focus the immune response toward desired, accessible epitopes, even in the presence of normally immunodominant epitopes. This has implications for filovirus DNA vaccines that contain epitopes conserved among several viruses, which could be used to boost otherwise subdominant antibody responses. Clearly, our study is limited by the small number of antibodies that we screened and the evaluation of only one multi-epitope construct. To gain a true appreciation of the utility of the screening methods that we used for designing a tailored DNA vaccine, it would be interesting to evaluate antibodies from studies in which animals were vaccinated with multiple filoviruses, monoclonal antibodies that are cross reactive among filoviruses, and combinations of antibodies.

## Methods

### Cell lines and virus propagation

COS-7 or Vero E6 cells were cultured in DMEM supplemented with 10% FBS and antibiotics (Penicillin/Streptomycin, 50 U/mL) at 37°C with 5% CO<sub>2</sub>. EBOV strain Mayinga was propagated in Vero E6 cells. When cells reached 90% confluency, the culture medium was removed and cells were infected under BSL4 conditions at an MOI of 0.01. After 1 hour, the inoculum was removed and fresh medium was added. The infected cultures were incubated at 37°C with 5% CO<sub>2</sub>. Cells were monitored daily for cytopathogenic effects (CPE) and when > 90% of the infected cells had detached from the culture vessel surface, the culture fluids were harvested, clarified by centrifugation and frozen at -80°C.

### Antibodies

The mouse mAbs used to screen the CLIPS libraries have been described in detail.<sup>6</sup> Briefly, all of the mAbs used in our studies

were previously shown to provide partial protection against EBOV challenge when passively transferred to BALB/c mice. mAbs 13F6 and 6E3 are in the same competitive binding group (Group 1), but have different isotypes (IgG1 or IgG2a, respectively). Neither of these mAbs neutralized EBOV in cell culture assays. mAbs 6D8 and 13C6 are in different competitive binding groups (2 and 4, respectively) and both were shown to neutralize EBOV in cell culture assays in the presence of complement. Control sera included in the screenings came from naïve mice or mice vaccinated with the empty plasmid as indicated in the text. Polyclonal sera tested included archived samples from previous studies. Guinea pig sera (107 and 130) came from animals vaccinated by gene gun with the EBOV GP DNA vaccine and boosted with recombinant baculovirus GP expression products.<sup>3</sup> This vaccine regimen provided partial protection against challenge with EBOV, but was not superior to vaccination with the DNA vaccine alone.<sup>3</sup> The mouse sera MUTC and MUTD came from animals vaccinated with DNA constructs in which one or the other of the 2 GP2 N-linked glycosylation sites were mutated as described previously<sup>14</sup> and as described in the text of this manuscript.

### Plasmids

All plasmid constructs in this study used the pWRG7077 vector described previously.<sup>23</sup> Constructs expressing WT GP or a selection of epitopes from the GP gene were codon-optimized for *Homo sapiens* and synthesized by GeneArt. Large-scale preparations of purified, research-grade plasmids were produced by Aldevron.

### CLIPS peptide libraries

CLIPS libraries were synthesized by Pepscan Systems (The Netherlands). The first library consisted of a total of 7,286 different CLIPS peptides divided into 14 groups to include: (1) All overlapping looped 15-mers, 1–662; (2) All overlapping linear 15-mers, 663–1324; (3) Combi double-looped 21-mers on T3 CLIPS, 1325–1580; (4) Combi triple-looped 32-mers on P2T3 CLIPS, 1581–2309; (5) Combi triple-looped 32-mers on P2T3 CLIPS, 2310–3038; (6) Combi triple-looped 32-mers on P2T3 CLIPS, 3039–3767; (7) Combi triple-looped 32-mers on P2T3 CLIPS, 3768–4279; (8) Combi triple-looped 32-mers on P2T3 CLIPS, 4280–4404; (9) Combi triple-looped 32-mers on P2T3 CLIPS, 4405–4620; (10) Combi triple-looped 32-mers on P2T3 CLIPS, 4621–5132; (11) Combi triple-looped 21-mers on P2T3 CLIPS, 5133–5757; (12) Combi triple-looped 21-mers on P2T3 CLIPS, 5758–6118; (13) Combi triple-looped 21-mers on P2T3 CLIPS, 6119–7142; (14) Combi triple-looped 21-mers on P2T3 CLIPS, 7143–7286 (Figure S1A). The second library was synthesized for fine mapping and included 3,750 34-mer CLIPS peptides to include: single-looped peptides on T2 scaffold, double-looped peptides on T3 scaffold, double-looped peptides on T2+T2 scaffold, triple-looped peptides on T2+T3 scaffold and sheet or helix-like peptides on T2+T2 scaffold (Figure S1B).

To probe the individual contributions of amino acids at certain positions, full substitution mutagenesis arrays were designed based on the initially retrieved leads. All peptides were synthesized on solid support and screened with varying

concentrations of antibody and blocking buffer to optimize signal-to-noise ratios in each experiment.<sup>5</sup>

### Mouse vaccinations with epitope-based DNA vaccines

Plasmid DNA was prepared at 25  $\mu\text{g}/20 \mu\text{l}$  in PBS. Groups of 6–8 week-old female BALB/c mice ( $N = 10$ ) were vaccinated 3 times at 3-week intervals with 20  $\mu\text{l}$  of DNA by intramuscular electroporation. Anesthetized mice were vaccinated in the tibialis anterior muscle using the Ichor Medical Systems Tri-Grid Delivery System.<sup>24</sup> Prior to each vaccination and at week 9, blood was collected and serum was isolated by centrifugation for ELISA.

### Immunofluorescence microscopy

COS-7 cells were cultured on 12 mm coverslips in 24-well plates under conditions described above. When cells reached 80% confluency, they were transfected with 1  $\mu\text{g}$  of purified plasmid DNA using Lipofectamine (Life Technologies). Twenty-four hours after transfection, medium was removed and the cells were washed with PBS and then fixed with 10% formalin. Cells were then permeabilized with PBS + 0.1% Triton-X for 5 minutes, washed with PBS, and blocked with PBS + 1% Tween 20 + 5% nonfat dried milk (NFDM). Next, cells were washed and incubated with mAb 6D8 (generously provided by John Dye, Jr.) for 1 hr. Finally, cells were washed, incubated with Alexa Fluor 488 goat anti-mouse IgG for 30 minutes, washed again, mounted onto slides with ProLong Gold Antifade reagent (Life Technologies) and imaged by fluorescence microscopy.

### Immunoblotting

COS-7 cells were transfected with plasmid DNA encoding WT GP, the multi-epitope construct, or empty vector. Cells were harvested, lysed in RIPA buffer and resolved on SDS-PAGE followed by transfer to PVDF for western blot. Western blotting was performed as per manufacturer's instructions using the Novex WesternBreeze Immunodetection kit. Primary antibody for these blots was mAb 6D8. Blots were blocked with 5% NFDM for 30 minutes, followed by 4 5-minute washes with PBST.

### ELISA

Gamma-irradiated, sucrose-purified EBOV virions were coated onto 96-well, flat-bottom plates at an optimized dilution of 1:1,000. Plates were then washed and blocked with PBST + 5% NFDM. Cell lysate or serum samples were initially diluted 1:100 in PBS and subsequently diluted 2-fold then applied to coated wells and incubated for 1 hr. Plates were then washed and incubated with HRP-conjugated goat anti-mouse secondary antibody (Promega). Next, plates were washed and ABTS substrate was added as per manufacturer's instructions (Pierce). Plates were then read on a microplate reader (Molecular Devices) and data was subsequently analyzed using Softmax pro software (Molecular Devices). Endpoint titers were determined

for each sample using a cutoff of 2 standard deviations above the signal observed in the negative control wells.

### Peptide ELISA

A library of biotinylated 18-mer peptides with a 6 amino acid overlap spanning the entire EBOV GP was constructed by Mimotopes (Raleigh, NC). These peptides served as coating antigens in our peptide ELISA. Each well of flat-bottom, 96-well assay plates was coated with a single peptide at a concentration of 2 mg/mL. Plates were then washed with PBST followed by blocking with PBST + 5% NFD. Plates were washed again and serum samples were applied at a 1:1,000 dilution. After incubation for 1 hr, plates were washed with PBS and HRP-conjugated goat anti-mouse secondary antibody (Promega) was applied and incubated for 1 hr. Finally, plates were washed with PBST, developed using ABTS substrate as per manufacturer's instructions (Pierce), and read on a microplate reader (Molecular Devices).

### Disclosure of potential conflicts of interest

No potential conflicts of interest were disclosed.

### Funding

Support for this research was provided by the Joint Science and Technology Office of the Defense Threat Reduction Agency, the Military Infectious Diseases Research Program of the United States (US) Army Medical Research and Materiel Command and the US Department of Defense (DoD) High-Performance Computing Modernization Program. These studies were performed while DM held a National Research Council Postdoctoral Fellowship at USAMRIID. The opinions, interpretations, conclusions, and recommendations contained herein are those of the authors and are not necessarily endorsed by the US Army.

### References

- [1] Grant-Klein RJ, Altamura LA, Badger CV, Bounds CE, Van Deusen NM, Kwilas SA, Vu HA, Warfield KL, Hooper JW, Hannaman D, et al. Codon-optimized filovirus DNA vaccines delivered by intramuscular electroporation protect cynomolgus macaques from lethal Ebola and Marburg virus challenges. *Hum Vaccines Immunotherapeutics*. 2015;11:1991-2004. doi:10.1080/21645515.2015.1039757
- [2] Grant-Klein RJ, Van Deusen NM, Badger CV, Hannaman D, Dupuy LC, Schmaljohn CS. A multiagent filovirus DNA vaccine delivered by intramuscular electroporation completely protects mice from ebola and Marburg virus challenge. *Hum Vaccines Immunotherapeutics*. 2012;8:1703-6. doi:10.4161/hv.21873
- [3] Mellquist-Riemenschneider JL, Garrison AR, Geisbert JB, Saikh KU, Heidebrink KD, Jahrling PB, Ulrich RG, Schmaljohn CS. Comparison of the protective efficacy of DNA and baculovirus-derived protein vaccines for EBOLA virus in guinea pigs. *Virus Res*. 2003;92:187-93. doi:10.1016/S0168-1702(02)00338-6. PMID:12686428
- [4] Corti D, Voss J, Gambelin SJ, Codoni G, Macagno A, Jarrossay D, Vachieri SG, Pinna D, Minola A, Vanzetta F, et al. A neutralizing antibody selected from plasma cells that binds to group 1 and group 2 influenza A hemagglutinins. *Science*. 2011;333:850-6. doi:10.1126/science.1205669. PMID:21798894
- [5] Timmerman P, Puijk WC, Meloen RH. Functional reconstruction and synthetic mimicry of a conformational epitope using CLIPS technology. *J Mol Recognition: JMR*. 2007;20:283-99. doi:10.1002/jmr.846. PMID:18074397

- [6] Wilson JA, Hevey M, Bakken R, Guest S, Bray M, Schmaljohn AL, Hart MK. Epitopes involved in antibody-mediated protection from Ebola virus. *Science*. 2000;287:1664-6. doi:10.1126/science.287.5458.1664. PMID:10698744
- [7] Dube D, Brecher MB, Delos SE, Rose SC, Park EW, Schornberg KL, Kuhn JH, White JM. The primed ebolavirus glycoprotein (19-kd-glycoprotein GP1,2): sequence and residues critical for host cell binding. *J Virol*. 2009;83:2883-91. doi:10.1128/JVI.01956-08. PMID:19144707
- [8] Schornberg K, Matsuyama S, Kabsch K, Delos S, Bouton A, White J. Role of endosomal cathepsins in entry mediated by the Ebola virus glycoprotein. *J Virol*. 2006;80:4174-8. doi:10.1128/JVI.80.8.4174-4178.2006. PMID:16571833
- [9] Chandran K, Sullivan NJ, Felbor U, Whelan SP, Cunningham JM. Endosomal proteolysis of the Ebola virus glycoprotein is necessary for infection. *Science*. 2005;308:1643-5. doi:10.1126/science.1110656. PMID:15831716
- [10] Kugelman JR, Kugelman-Tonos J, Ladner JT, Pettit J, Keeton CM, Nagle ER, Garcia KY, Froude JW, Kuehne AI, Kuhn JH, et al. Emergence of Ebola virus escape variants in infected non-human primates treated with the MB-003 antibody cocktail. *Cell Reports*. 2015;12:2111-20. doi:10.1016/j.celrep.2015.08.038. PMID:26365189
- [11] Olal D, Kuehne AI, Bale S, Halfmann P, Hashiguchi T, Fusco ML, Lee JE, King LB, Kawaoka Y, Dye JM, Jr, et al. Structure of an antibody in complex with its mucin domain linear epitope that is protective against Ebola virus. *J Virol*. 2012;86:2809-16. doi:10.1128/JVI.05549-11. PMID:22171276
- [12] Warfield KL, Swenson DL, Olinger GG, Nichols DK, Pratt WD, Blouch R, Stein DA, Aman MJ, Iversen PL, Bavari S. Gene-specific countermeasures against Ebola virus based on antisense phosphorodiamidate morpholino oligomers. *PLoS Pathogens*. 2006;2:e1. doi:10.1371/journal.ppat.0020001. PMID:16415982
- [13] Geisbert TW, Hensley LE, Jahrling PB, Larsen T, Geisbert JB, Paragas J, Young HA, Fredeking TM, Rote WE, Vlasuk GP. Treatment of Ebola virus infection with a recombinant inhibitor of factor VIIa/tissue factor: a study in rhesus monkeys. *Lancet*. 2003;362:1953-8. doi:10.1016/S0140-6736(03)15012-X. PMID:14683653
- [14] Dowling W, Thompson E, Badger C, Mellquist JL, Garrison AR, Smith JM, Paragas J, Hogan RJ, Schmaljohn C. Influences of glycosylation on antigenicity, immunogenicity, and protective efficacy of ebola virus GP DNA vaccines. *J Virol*. 2007;81:1821-37. doi:10.1128/JVI.02098-06. PMID:17151111
- [15] Vanderzanden L, Bray M, Fuller D, Roberts T, Custer D, Spik K, Jahrling P, Huggins J, Schmaljohn A, Schmaljohn C. DNA vaccines expressing either the GP or NP genes of Ebola virus protect mice from lethal challenge. *Virology*. 1998;246:134-44. doi:10.1006/viro.1998.9176. PMID:9657001
- [16] Lee JE, Fusco ML, Hessel AJ, Oswald WB, Burton DR, Saphire EO. Structure of the Ebola virus glycoprotein bound to an antibody from a human survivor. *Nature*. 2008;454:177-82. doi:10.1038/nature07082. PMID:18615077
- [17] Howell KA, Brannan JM, Bryan C, McNeal A, Davidson E, Turner HL, Vu H, Shulenin S, He S, Kuehne A, et al. Cooperativity enables Non-neutralizing antibodies to neutralize Ebola virus. *Cell Reports*. 2017;19:413-24. doi:10.1016/j.celrep.2017.03.049. PMID:28402862
- [18] Keck ZY, Enterlein SG, Howell KA, Vu H, Shulenin S, Warfield KL, Froude JW, Araghi N, Douglas R, Biggins J, et al. Macaque monoclonal antibodies targeting novel conserved epitopes within filovirus glycoprotein. *J Virol*. 2015;90:279-91. doi:10.1128/JVI.02172-15. PMID:26468532
- [19] Davidson E, Bryan C, Fong RH, Barnes T, Pfaff JM, Mabila M, Rucker JB, Doranz BJ. Mechanism of binding to Ebola virus glycoprotein by the ZMapp, ZMAb, and MB-003 cocktail antibodies. *J Virol*. 2015;89:10982-92. doi:10.1128/JVI.01490-15. PMID:26311869
- [20] Murin CD, Fusco ML, Bornholdt ZA, Qiu X, Olinger GG, Zeitlin L, Kobinger GP, Ward AB, Saphire EO. Structures of protective antibodies reveal sites of vulnerability on Ebola virus. *Proc Natl Acad Sci U S A*. 2014;111:17182-7. doi:10.1073/pnas.1414164111. PMID:25404321
- [21] Tran EE, Nelson EA, Bonagiri P, Simmons JA, Shoemaker CJ, Schmaljohn CS, Kobinger GP, Zeitlin L, Subramaniam S, White JM.

- Mapping of Ebolavirus neutralization by monoclonal antibodies in the ZMapp cocktail using Cryo-electron tomography and studies of cellular entry. *J Virol.* 2016;90:7618-27. doi:10.1128/JVI.00406-16. PMID:27279622
- [22] Pallesen J, Murin CD, de Val N, Cottrell CA, Hastie KM, Turner HL, Fusco ML, Flyak AI, Zeitlin L, Crowe JE, Jr, et al. Structures of Ebola virus GP and sGP in complex with therapeutic antibodies. *Nature Microbiol.* 2016;1:16128. doi:10.1038/nmicrobiol.2016.128. PMID:27562261
- [23] Schmaljohn C, Vanderzanden L, Bray M, Custer D, Meyer B, Li D, Rossi C, Fuller D, Fuller J, Haynes J, et al. Naked DNA vaccines expressing the prM and E genes of Russian spring summer encephalitis virus and Central European encephalitis virus protect mice from homologous and heterologous challenge. *J Virol.* 1997;71:9563-9; PMID:9371620
- [24] Luxembourg A, Hannaman D, Ellefsen B, Nakamura G, Bernard R. Enhancement of immune responses to an HBV DNA vaccine by electroporation. *Vaccine.* 2006;24:4490-3. doi:10.1016/j.vaccine.2005.08.014. PMID:16140436
- [25] Lee JE, Kuehne A, Abelson DM, Fusco ML, Hart MK, Saphire EO. Complex of a protective antibody with its Ebola virus GP peptide epitope: unusual features of a V lambda x light chain. *J Mol Biol.* 2008;375:202-16. doi:10.1016/j.jmb.2007.10.017. PMID:18005986